

# Mapping surface sources of acid mine drainage using remote sensing: case study of the Witbank, Ermelo and Highveld coalfields

Emmanuel Sakala<sup>1,2</sup>, Francois Fourie<sup>2</sup>, Modreck Gomo<sup>2</sup>, Henk Coetzee<sup>1</sup>

<sup>1</sup>*Council for Geoscience, Private Bag X112, Pretoria, 0001, South Africa, esakala@geoscience.org.za*

<sup>2</sup>*Institute of Groundwater Studies, University of the Free State, PO Box 339, Bloemfontein, 9300, South Africa*

**Abstract** The research involves formulating a methodology to automatically map surface acid mine drainage pollutant sources using remote sensing in support of environmental and coal discard management in the Witbank, Ermelo and Highveld coalfields. The spectral uniqueness of acid mine drainage-generated secondary iron-bearing minerals is used to build a decision tree for differentiating these from other minerals depicted from Landsat 8 data. Previously known acid mine drainage-generating coal discard dumps coincide with the remote sensing mapped minerals (jarosite and haematite). The mapped acid mine drainage sources can be used to plan management and mitigation strategies for the protection of water resources.

**Key words** Acid mine drainage, coalfield, remote sensing, mineral, pollutant source

## Introduction

Acid mine drainage (AMD) is formed when sulfide minerals (pyrite and marcasite) emanating from coal mining operations or orebodies are oxidised by water in the presence of oxygen to form an acidic solution (Pinetown et al., 2007). The AMD formed is characterised by low pH values, high concentrations of sulfate and total dissolved solids (TDS), and elevated concentrations of heavy metals, such as iron, aluminium and manganese, which are remobilised by the acidic environment (Bell et al., 2001). Elevated concentrations of these substances in water resources cause a deterioration of the water quality, adversely affecting aquatic life and posing serious health concerns to humans and animals. The deposition of various secondary iron minerals (Fe-bearing) is also typically associated with AMD (Bell et al., 2001). Sources of AMD range from surface exposed sources (mine discards, tailing dumps, coal loading bays, coal washing plants) to sources buried within the subsurface (coal orebodies). The potential AMD sources in the subsurface are usually starved of oxygen (a key ingredient in AMD generation) and therefore pose little risk as AMD sources. This paper proposes a cost-effective methodology to map surface AMD sources over large areas (coalfield or catchment scale) using remote sensing data.

There are nineteen coalfields in South Africa, with the current mining activities largely taking place in the Witbank, Ermelo and Highveld coalfields located in the Mpumalanga Province of South Africa (Banks et al., 2011). These coalfields are located between latitude 25°30' to 27°45' south and longitude 28°30' and 30°30' east, covering an area of approximately 23 315 km<sup>2</sup> (fig. 1). The area receives an average long-term rainfall of between 600 and 1 100 mm (SAWS 2016). The winters are typically dry and cold with occasional frost, while the

summers, between October and March, are hot (Barnard 2000). Coal mining within these coalfields has polluted several areas and cause of concern for local communities in recent years (McCarthy and Pretorius 2009).

The Witbank, Highveld and Ermelo coalfields comprise multiple seam deposits with the development of up to five major coal seam horizons which may, in places, be composite seams. Coal is hosted in the Ecca Group of the Karoo Supergroup which dates back to the Permian period between 280 and 250 Ma. The Ecca Group consists of sandstone, siltstone, mudstone and shales (Cairncross et al., 1990). Coal is mainly mined by open-cast methods because the resources are shallow, largely unfaulted and slightly inclined (CMSA 2017). The coalfields have been mined for over a century, which has caused several AMD-generating strata to become exposed to water and oxygen. In order to ensure environmental mitigation on a coalfield scale, the exposed AMD potential sources need to be identified.

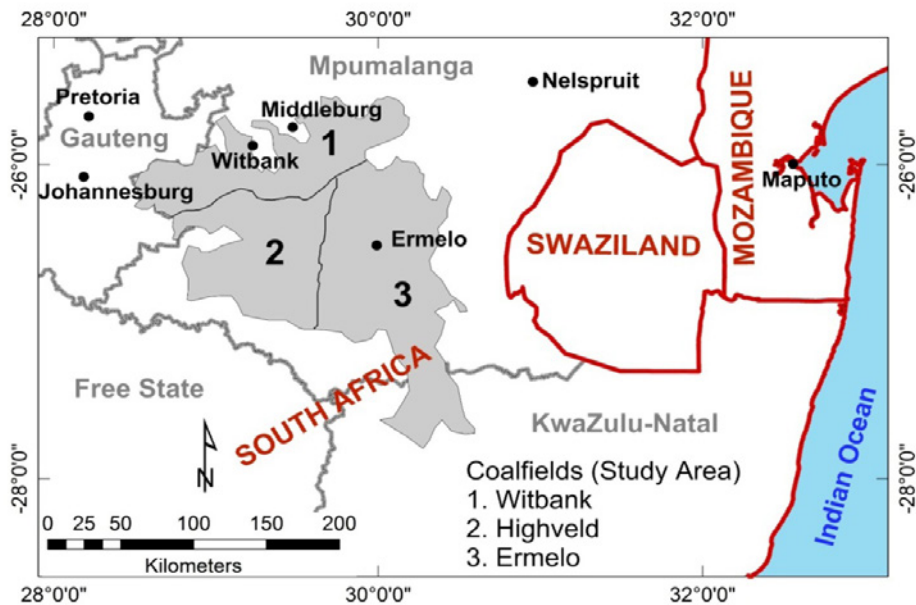


*Figure 1* Location of study area in South Africa.

## Methods

The methodology used for the identification of AMD sources from Landsat 8 remote sensing data involves the following processes:

- Identification of the spectral signature of Fe-bearing minerals in mine discard dumps within the study area. Identification can be done by taking several spectral readings of the mine discard dumps using a handheld spectroradiometer or extracting spectral data from the USGS mineral spectral library. The Fe-bearing minerals are indicators of the geochemical environment in which they were formed. The commonly known Fe-bearing minerals which are

sensitive indicators of pH, Eh, relative humidity, degree of oxidation and other environmental conditions are copiapite ( $\text{Fe}^{+2} \text{Fe}_4^{+3}(\text{SO}_4)_6(\text{OH})_2 \cdot 20(\text{H}_2\text{O})$ ), jarosite ( $\text{KFe}_3^{+3}(\text{SO}_4)_2(\text{OH})_6$ ), schwertmannite ( $\text{Fe}_{16}^{+3}\text{O}_{16}(\text{SO}_4)_2(\text{OH})_{12} \cdot n\text{H}_2\text{O}$  ( $n \sim 10$  to  $12$ )), ferrihydrite ( $5\text{Fe}_2\text{O}_3 \cdot 9\text{H}_2\text{O}$ ), goethite ( $\text{Fe}^{+3}\text{O}(\text{OH})$ ) and haematite ( $\text{Fe}_2\text{O}_3$ ) (Swayze et al., 2000; Crowley et al., 2003). Within the study area, the Fe-bearing minerals which form in abundance are haematite and jarosite, according to a study by Cole et al. (2015). The spectral uniqueness of these Fe-bearing minerals makes it possible to identify them from orbital and airborne imaging data.

- Resampling of the mineral spectral data to Landsat 8 bandwidth sizes.
- Comparison of various bands and identification of the reflectance value differences to be used in order to differentiate between the AMD indicator minerals and the other minerals present.
- Developing a decision tree for differentiating various minerals using their reflectance responses at various bandwidths. The decision tree is then applied to the Landsat 8 data to produce a map showing the distribution of the AMD indicator minerals.
- Verification of the results by follow-up ground investigations over the identified AMD sources.

In this paper, free Landsat 8 data downloaded from the USGS website were used to identify secondary Fe-bearing minerals. Landsat 8 data comprise nine bands in the visible and near-infrared (VNIR) and short-wave infrared (SWIR) ranges (Band 8 is the panchromatic band and Band 9 is a cloud detection band) and two bands in the thermal infrared (TIR) range (table 1).

**Table 1** Properties of Landsat 8 data used (Cole et al., 2015).

Range	Band	Wavelength range (nm)	Spatial resolution (m)
VNIR	1	433–453	30
	2	450–515	30
	3	525–600	30
	4	630–680	30
	5	845–885	30
	8	500–680	15
SWIR	6	1 560–1 660	30
	7	2 100–2 300	30
	9	1 360–1 390	30
TIR	10	10 600–11 200	100
	11	11 500–12 500	100

The downloaded Landsat 8 data in digital numbers (DN) value format were first converted to reflectance values using the following equation (USGS 2016):

$$\text{Reflectance} = (MQ) + A \quad (1)$$

Where, M is the band-specific multiplicative rescaling factor, Q represents the quantised and calibrated standard product pixel values and A is the band-specific additive rescaling factor.

Clouds, cloud shadows and vegetation were masked out of the reflectance data to obviate the creation of a false classification when running the minerals mapping process. In this study, the spectral signatures of all the secondary Fe-bearing minerals were extracted from the USGS spectral library (Clark et al., 2007). The spectral signature of jarosite and haematite from the USGS spectral library reveals that these two minerals show unique reflectance signatures which can be used to distinguish between them and other minerals (fig. 2).

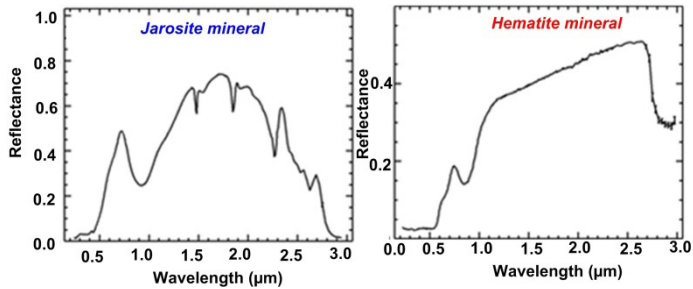


**Figure 2** Spectral signature of Fe-bearing minerals extracted from the USGS spectral library (Clark et al., 2007).

The spectral signatures of all the Fe-bearing minerals were resampled to the detection ranges of Landsat 8 bands. The resampled spectral signatures of jarosite and haematite still show their distinct spectral signatures (fig. 3).

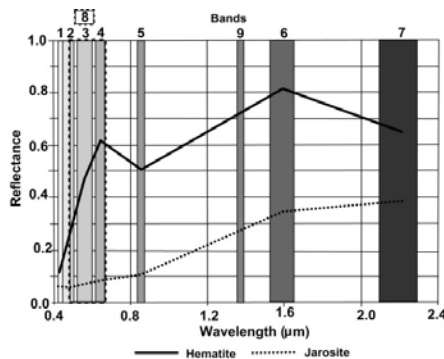


**Figure 3** Secondary Fe minerals spectrum resampled to Landsat 8 bandwidths (After Cole et al., 2015).

Based on the resampled spectrum of jarosite (fig. 3), the reflectance value for Band 5 is lower than that of Band 4, but not for the other bands. For haematite, Band 7 is greater than Band 6 and is thus distinguishable from the value recorded for jarosite. This spectral uniqueness of the minerals was used to create a decision tree (fig. 4) to identify these minerals using Landsat 8 reflectance data. The decision tree was implemented in ArcGIS and the AMD-related secondary Fe-bearing zones were identified within the study area.

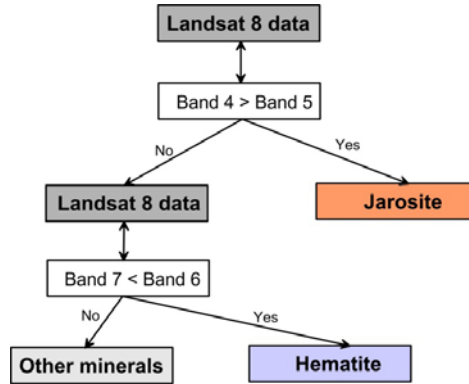


Figure 4 Decision tree used to identify secondary Fe minerals from Landsat 8 data.

**Results and discussions**

Areas where mine residue occurs show up in grey on the Landsat 8 band combination (Band 7 in red, Band 6 in blue and Band 4 in green), water appears bluish and vegetation appears green (fig. 5a). Not all mine residue dumps are acid generating and only those that are indeed acid generating will precipitate the secondary Fe minerals and thus be identifiable using this approach. After implementing the decision tree in a GIS environment; Landsat 8 data covering the whole study area were used to produce a map showing only the interpreted Fe-bearing minerals which can be used as potential AMD surface sources (fig. 5b).

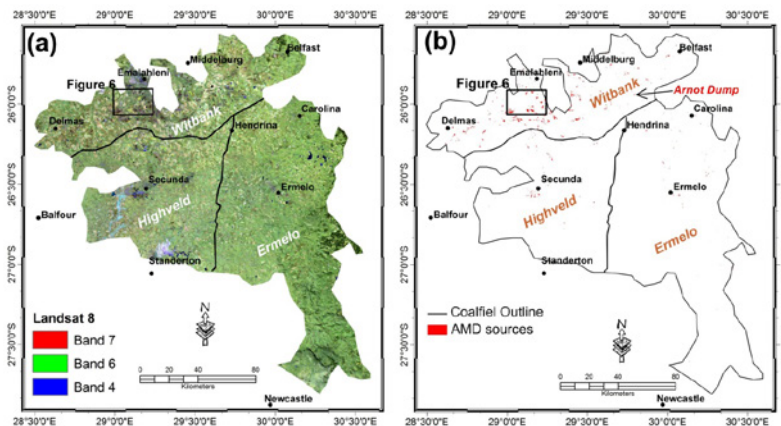
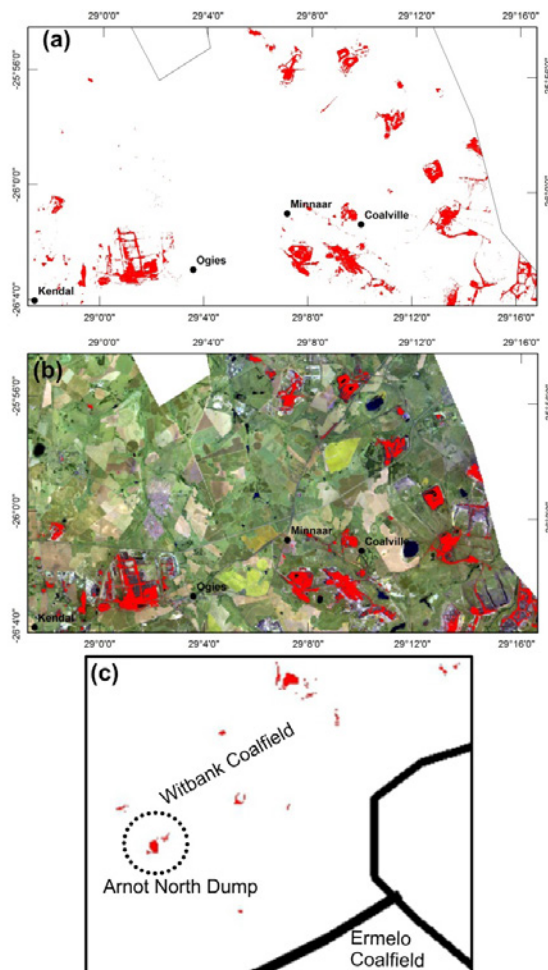


Figure 5 (a) Landsat 8 band combination 764 image (b) extracted secondary Fe minerals.

A small section of the Witbank coalfield was selected for a detailed analysis of the results. The interpreted jarosite and haematite minerals are shown in red (fig. 6a). The area lies south of eMalahleni and covers the Kendal, Ogies, Minnaar and Coalville areas (fig. 6a). When the interpreted results are overlain onto the Landsat 8 band combination, it can be seen that the mapped jarosite and haematite minerals coincide with some mine discard areas and a coal loading terminal (fig. 6b). Several mine discard dumps in the Witbank coalfield were identified as acid generating in a study conducted by Nohve et al.. (2013) correspond to the mapped jarosite and haematite minerals. The Witbank coalfield has the highest density of interpreted AMD surface sources while the Ermelo coalfield has the lowest density. This finding is in agreement with the literature which states that the Witbank coalfield currently is the highest producer of coal while the Ermelo coalfield is the lowest (Bell et al.. 2001; Hobbs et al.. 2008).



**Figure 6** Zoomed-in results (a) Fe minerals; (b) Landsat 8 band combination 764 for a detailed

*analysis of interpreted secondary Fe minerals; (c) Arnot North discard mine dump.*

To test the validity of the identified AMD sources, the mine discard dumps classified as AMD sources in this paper were compared with the dumps identified as acid generating by Novhe et al. (2013). Novhe et al. (2013) had used static tests including paste pH, a neutralisation analysis, acid potential determination and kinetic tests (column leach tests) to identify AMD generating mine discard dumps in the Witbank coalfield. Consequently, the Arnot North mine discard dump was identified as acid generating. Moreover, the site is characterised by high secondary Fe-bearing minerals (fig. 6c). The results from the remote sensing technique are in agreement with laboratory tests, thus increasing confidence in the usage of remote sensing data.

## Conclusions

The paper describes the application of a remote sensing technique which can be used by environmental agencies to quickly select potential AMD generating mine discard dumps thereby improving decision making in respect of the implementation of mitigation measures. Selection of secondary Fe-bearing minerals from aerial Landsat 8 aerial data ensured that most of these minerals occurring in waste rocks and mine dumps and those that have been transported and deposited on roads, railway lines, loading bays, wetlands and river banks are all mapped at a 30 m resolution. The mapped AMD pollutant sources can be used by mining authorities and environmental agencies to plan management and mitigation measures to prevent the AMD from reaching water resources. The approach can be extended to other high resolution aerial remote sensing data to increase the spatial resolution once the data becomes accessible freely or at lower cost.

## References

- Banks VJ, Palumbo-Roe, Van Tonder DB, Davies J, Fleming C and Chevrel S (2011) Conceptual models of the Witbank coalfield, South Africa. Earth observation for monitoring and observing environmental and societal impacts of mineral resources exploration and exploitation, cEC FP7 Project EO-MINERS, Deliverable D3. 1–2, 107.
- Barnard HC (2000) An explanation of the 1:500 000 general hydrogeological map-Johannesburg 2526, Department of Water and Sanitation.
- Bell FG, Bullock SET, Halbich TFJ and Lindsay P (2001) Environmental impacts associated with an abandoned mine in the Witbank coalfield, South Africa. *International Journal of Coal Geology* 45, 195–216.
- Cairncross B, Hart RJ and Willis JP (1990) Geochemistry and sedimentology of coal seams from the Permian Witbank Coalfield, South Africa: a means of identification. *International Journal of Coal Geology*, 16, 309–325.
- Chamber of Mines of South Africa (CMSA) (2017) Mining in SA: Coal <<http://www.chamberofmines.org.za/sa-mining/coal>> Accessed: 09 April 2017.
- Clark RN, Swayze GA, Wise R, Livo E, Hoefen T, Kokaly R and Sutley SJ (2007) USGS digital spectral library splib06a: U.S. Geological Survey, Digital Data Series 231, <<http://speclab.cr.usgs.gov/spectral.lib06>>
- Cole J, Cole P, Yibas B, Vadapalli V, Novhe O and Netshitungulwana R (2015) A holistic approach towards best management of mine pollution impacts on water resources of South Africa

- using river catchment strategy: Report on remote sensing for mining pollution & AMD, Council for Geoscience, unpublished report No 2015-0092.
- Crowley JK, Williams DE, Hammarstrom JM, Piatak N, Chou IM and Mars JC (2003) Spectral reflectance properties (0.4–2.5 m) of secondary Fe-oxide, Fe-hydroxide, and Fe-sulphate-hydrate minerals associated with sulphide-bearing mine wastes. *Geochemistry: Exploration, Environment and Analysis* 3(3), 219–228.
- Hobbs P, Oelofse S, Rascher J (2008) Management of environmental impacts from coal mining in the Upper Olifants River Catchment as a function of age and scale. *Water Resources Development*, 24(3), 417–431.
- McCarthy TS and Pretorius K (2009) Coal mining on the Highveld and its implications for future water quality in the Vaal river system. *International Mine Water Conference Proceedings*, Pretoria, South Africa, p 56–65.
- Novhe NO, Maree J, Ogola JS (2013) Characterization of potential acid leachate from raw coal, discard coal and slimes from a colliery in the Witbank Coalfield, Mpumalanga Province, South Africa. *International Mine Water Conference Proceedings*, Golden CO, United States, 875–880.
- Pinetown KL, Ward CR and van der Westhuizen WA (2007) Quantitative evaluation of minerals in coal deposits in the Witbank and Highveld coalfields, and the potential impact on acid mine drainage. *International Journal of Coal Geology* 70, 166–183.
- South African Weather Service (SAWS) (2016) Historical Rain Maps, <<http://www.weathersa.co.za/climate/historical-rain-maps>> Accessed: 23 March 2016.
- Swayze GA, Smith KS, Clark RN, Sutley SJ, Pearson RM, Vance JS, Hageman PL, Briggs PH, Meier AL, Singleton MJ and Roth S (2000) Using imaging spectroscopy to map acidic mine waste, *Environmental Science and Technology* 34, 47–54.
- United State Geological Survey (USGS) (2016) Earth Explorer-Landsat 8, <[www.earthexplorer.usgs.gov](http://www.earthexplorer.usgs.gov)>, Accessed: 30 March 2016.